Immunoassays in Nanoliter Volume Reactors Using Fluorescent Particle Diffusometry

ARTICLE *in* LANGMUIR · APRIL 2008

Impact Factor: 4.46 · DOI: 10.1021/la703224b · Source: PubMed

4 AUTHORS, INCLUDING:

Gil U Lee
University College Dublin
107 PUBLICATIONS **4,291** CITATIONS

SEE PROFILE

Immunoassays in Nanoliter Volume Reactors Using Fluorescent Particle Diffusometry

Venu M. Gorti,[‡] Hao Shang,[†] Steven T. Wereley,[‡] and Gil U. Lee*,[†]

Schools of Chemical and Biomedical Engineering and School of Mechanical Engineering, Purdue University, West Lafayette, Indiana 47907

Received October 16, 2007. In Final Form: December 11, 2007

A model analyte, the M13 virus, was detected through the change in the Brownian motion of a population of microparticles. Epi-fluorescence microscopy was used to simultaneously track antibody-coated and bare microparticles to unambiguously measure the diffusion coefficient and demonstrate multiplexed detection. The sensitivity of the diffusometry assay was high enough that individual virus-to-particle binding ratios could be detected. Analysis of the experimental errors indicated that the primary limitation in the sensitivity of this technique was the variation in the size of the population of microparticles. Analysis of the diffusion measurement results indicated that the change in the drag coefficient of the virus−particle assembly was not a simple sum of the drag coefficients of the individual components and the rate of particle−particle reaction was slower than would be predicted from the uncoupled particle hydrodynamics. The possibility of using diffusometry for sensing and proteomics applications is examined.

Introduction

The availability of genetic information for many organisms has created a need for bioanalytical technologies that are capable of simultaneously determining the concentration of the thousands of proteins that make up cells.[1,2] Proteomic and genomic analysis is currently dominated by two approaches. Micrometer-scale solid-phase assays are now widely used to characterize protein and RNA/DNA expression levels.[3,4] In these assays, large numbers of oligonucleotides or proteins are placed in an addressable array on a substrate, reacted with a sample, and read out with fluorescent (or colorimetric) imaging. Microarrays are now routinely used for simultaneously characterize the concentration of thousands of oligonucleotides at a sensitivity that exceeds 1 nM. The second widely accepted approach to proteomic and genomic analysis involves mass spectrometry, which is typically used in conjunction with electrophoresis or liquid chromatography.[5−8] The advantage of this approach is that molecular receptors do not have to be available for a large number of analytes, and post-translational modification and protein−protein interactions can be identified. There is currently a need for protein (and RNA/DNA) assays that have higher sensitivities, have quicker response times, and are capable of working with smaller volumes of material.

In this study we use the reaction of an analyte with micrometer-size particles functionalized with antibodies and resulting change in their Brownian motion to determine the analyte concentration. The advantages of this technique are that it requires only a single receptor, the rate of reaction allows the assay to be completed in 35 min, the total volume of analysis is less than a nanoliter, and the sensitivity can reach a single molecule per particle. This technical advance suggests that particle diffusometry could be implemented to simultaneously characterize a large number of analytes contained in microfabricated arrays of nanoreactors that are integrated with a mesomembrane.[9] Figure 1 presents an optical micrograph of an array of plastic reactors of three volumes that are supported on a 60 μm thick alumina membrane with a minimum pore size of 20 nm. We have recently demonstrated that biochemical reactions can be preformed through this mesoporous membrane[9] and that inkjet arraying can be used to deposit specific analytes in the specific microreactors in the array.[10]

Advances in optical microscopy have made it possible to simultaneously track and analyze the motion of thousands of microparticles, and particle-imaging velocimetry is now commonly used to study flow in microfabricated devices.[11] In this study we focus on demonstrating that diffusometry can be used to detect an immunochemical reaction and define the experimental variables that determine the sensitivity and speed of the technique. The M13 virus has been used as a model analyte because it has a well-defined size and it is large enough to allow micrometer-size microparticles to be used, which are readily available and easy to use. As expected, the binding of the virus decreases the diffusion coefficient of the microparticle by increasing the drag coefficient of the virus−microparticle assembly. The drag coefficient of the virus−microparticle assembly was studied to determine if the number of viruses bound to the particle can be determined and the impact of environmental variables on the change in this diffusion coefficient. Two-color diffusometry was introduced and it was demonstrated that it can be used to minimize the influence environmental variables, such as temperature, particle concentration, and viscosity.

Materials and Methods

Preparation of Antibody-Functionalized Microparticles. Green and red fluorescent microparticles were acquired from a commercial

* To whom correspondence should be addressed. E-mail: gl@ecn.purdue.edu.

† Schools of Chemical and Biomedical Engineering.

‡ School of Mechanical Engineering.

(1) Aach, J.; Bulyk, M. L.; Church, G. M.; Comander, J.; Derti, A.; Shendure, J. *Nature* **2001**, *409*, 856−859.

(2) Consortium, I. H. G. S. *Nature* **2001**, *409*, 860−921.

(3) Fodor, S. P. A.; Read, J. L.; Pirrung, M. C.; Stryer, L.; Lu, A. T.; Solas, D. *Science* **1991**, *251*, 767−773.

(4) Pease, A. C.; Solas, D.; Sullivan, E. J.; Cronin, M. T.; Holmes, C. P.; Fodor, S. P. A. *Proc. Natl. Acad. Sci. U.S.A.* **1994**, *91*, 5022−5026.

(5) Yamashita, M.; Fenn, J. B. *J. Phys. Chem.* **1984**, *88*, 4451−4459.

(6) Fenn, J. B.; Mann, M.; Meng, C. K.; Wong, S. F.; Whitehouse, C. M. *Science* **1989**, *246*, 64−71.

(7) Tanaka, K.; Waki, H.; Ido, Y.; Akita, S.; Yoshida, Y.; Yoshida, T. *Rapid Commun. Mass Spectrosc.* **1988**, *2*, 151−153.

(8) Aebersold, R.; Mann, M. *Nature* **2003**, *422*, 198−207.

(9) Wang, Z. G.; Haasch, R. T.; Lee, G. U. *Langmuir* **2005**, *21*, 1153−1157.

(10) Wang, Z. G.; Shang, H.; Lee, G. U. *Langmuir* **2006**, *22*, 6723−6726.

(11) Meinhart, C. D.; Wereley, S. T.; Santiago, J. G. *Exp. Fluids* **1999**, *27*, 414−419.

10.1021/la703224b CCC: $40.75
Published on Web 02/23/2008

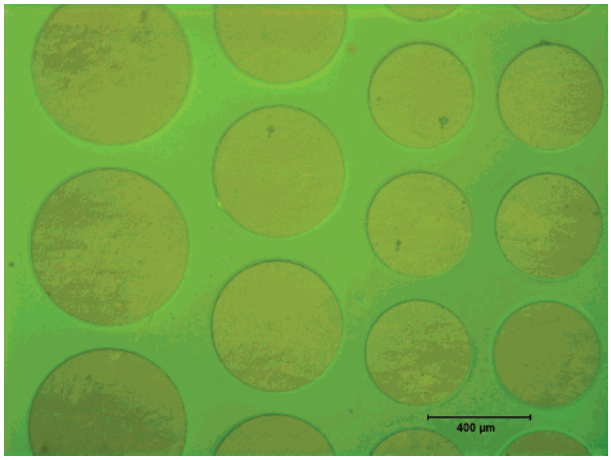

Figure 1. Optical micrograph of plastic reactors that have been microfabricated on a mesoporous alumina membrane. The volume of the 400 μm diameter reactor is 5 nL. Previous studies have demonstrated that these rugged structures[28] have a permeability is consistent with 20 nm size pores[9] and can be functionalized with an inkjet arrayer.[10]

supplier (Duke Scientific, Fremont, CA) that were made of polystyrene. The green microparticles had a manufacturer specified diameter of 0.71 μm, excitation maxima at 468 nm, and emission maxima at 508 nm. The red microparticles had a manufacturer specified diameter of 0.69 μm, excitation maxima at 542 nm, and emission maxima at 612 nm.

The red particles were functionalized with antibodies using a poly(ethylene glycol) (PEG) hetrobifunctional grafting surface chemistry that is illustrated in Figure 2.[12] A 150 μL aliquot of stock particle solution, containing 7.5×10^9 particles, was washed in 50 mM of carbonate buffer, pH 8.2, three times. After the last wash, the particles were resuspended by sonication in 1 mL of 5% polyethylene imine (PEI, Polymin SNA, BASF, Rensseler, NY) in carbonate buffer (Figure 2B). These particles were functionalized with a vinyl-sulfone PEG monolayer by reacting α-vinyl sulfone, *ω-N*-hydroxysuccinimidyl ester of poly(ethylene glycol)−propionic acid (NHS-PEG-VS) (Nektar, Huntsville, AL) with the PEI-coated particles (Figure 2C).

Antibodies against the pVIII protein of the M13 virus were obtained from Pharmacia (Piscataway, NJ), and the M13 virus was obtained from New England BioLabs Inc. (Beverly, MA). The anti-pVIII antibody was activated with sulfhydryl groups using *N*-succinimidyl-*S*-acetylthioacetate (SATA) (Pierce Biotechnology, Rockford, IL) in a 1:10 molar ratio in 50 mM phosphate buffer with 1 mM EDTA at pH 7.5 for 30 min. The sulfhydryl groups on the SATA antibody were deprotected in a deacetylation buffer of 62.5 mM Na_2HPO_4/NaH_2PO_4, 50 mM hydroxylamine HCl, and 2.5 mM EDTA at pH 7.5 for 2 h. Excess SATA and deacetylation buffer were removed by ultrafiltration (Microcon 30, Millipore, Billerica, MA). The concentration of antibodies was determined by micro-BCA assay (Pierce). The activated antibody was reacted with the PEG−VS-coated particles in 50 mM phosphate buffer and 1 mM EDTA, pH 7.2 on a rotating wheel for 3 h. The sulfhydryl group on the antibodies reacted specifically with the vinyl sulfone on the PEG, Figure 1D. The antibody-functionalized particles were separated from the solution and washed three times with PBS (12 mM phosphate buffer with 150 mM NaCl) and resuspended in 1 mL of PBS.

Optical Microscope and Particle Tracking Algorithm. An inverted optical microscope (TE200, Nikon, USA) equipped with fluorescein−isothiocyanate (FITC) and tetramethylrhodamine−isothiocyanate (TRITC) filter cubes was used to image the microparticles in epi-fluorescence mode. The objective lens was used with magnification of 20× and a numerical aperture of 0.45, resulting in a depth of field of ∼3.5 μm. Digital images were captured with an interline transfer charge-coupled device (CCD) camera (Coolsnap HQ, Photometrics, Roper Scientific, Inc.). This camera had a 1392 × 1040 pixel array with a 6.45 μm × 6.45 μm pixel pitch. The exposure time was set at 10 ms, and the time between images was 300 ms. Suspensions of 4.6×10^8 particles/mL were observed in the microreactors. The reactors were fabricated on glass and coated with a monolayer of bovine serum albumin (BSA) to minimize the adsorption of the particles to the walls of the reactor. By switching between the filter cubes, the green and red particles could be selectively imaged.

Typically, 700 frames of particle motion were acquired at a rate of 300 ms/frame in an object plane that was approximately at the center of the rector. Image acquisition was controlled using Metamorph (Universal Imaging Corp., PA). These images had about 10−20 particles per image. Each frame was analyzed, and the local brightness maxima were identified as candidate particles. Two conditions were used to identify particles for analysis: (1) the maxima were no closer than 10 particle diameters from the nearest maxima and (2) a brightness threshold was used that required the maximum intensity to be in the upper 30th percentile of brightness of the image. The intensity matrix around a maximum was extracted and a Gaussian function described by

$$I(x, y) = Ae^{-((x-\mu_x)^2+(y-\mu_y)^2)/2\sigma^2} \quad (1)$$

was fit over the intensity distribution. This approach provided the center location of each particle in an image with an error of less than a tenth of a pixel.[13] Figure 3 presents a sample image. The particles identified in red were those selected for analysis, according to the criteria described above.

The particles were tracked over the set of 700 frames for as long as they adhered to the constraints described above. The center of the particles was used to determine the particle displacement over the 300 ms period. For each time step, the displacement data formed a Gaussian distribution whose variance increased linearly with time. The mean square displacement of a particles, $\langle s^2 \rangle$, over a period of time, Δt, has been defined by Langevin and Einstein[14] to be

$$\langle s^2 \rangle = 2ND\Delta t \quad (2)$$

where N is the number of translational degrees of freedom and D is the diffusion coefficient. The diffusion coefficient of the microparticles was determined from the mean square displacement of a particles where $N = 2$.

Results

The interaction of the M13 virus with the antibody-coated microparticles was characterized by electron microscopy. The M13 virus was reacted with 0.69 μm diameter anti-pVIII antibody-coated particles at a density of 9.2×10^8 particles/mL for 30 min in PBS. Figure 4 presents a typical TEM image in which the M13 virus was reacted with the microparticles at a 10:1 ratio. The large black circular structure in the middle of the image is the microparticle. Multiple viruses can be seen surrounding the microparticle. The M13 is a filamentous phage that is ∼6.5 nm in diameter and 930 nm in length, containing a circular single-stranded DNA genome encased in a long protein capsid.[15] In this specific image the filamentous M13 are attached to the particle through the pVIII protein. pVIII is a 50-amino-acid protein that makes up the capsid of the virus, and thus, there are ∼2700 molecules along the major axis of the virus. The TEM images suggest that a significant fraction of the phage extend at almost

(12) Lee, G. U.; Metzger, S.; Natesan, M.; Yanavich, C.; Dufrene, Y. F. *Anal. Biochem.* **2000**, *287*, 261−271.

(13) Crocker, J. C.; Grier, D. G. *J. Colloid Interface Sci.* **1996**, *179*, 298−310.

(14) Einstein, A. *Investigation on the Theory of Brownian Movement*; Dover: New York, 1956.

(15) Fields, B. N.; Knipe, D. M.; Howley, P. M. *Fields' Virology*, 5th ed.; Wolters Kluwer Health/Lippincott Williams and Wilkins: Philadelphia, 2007; p 2.

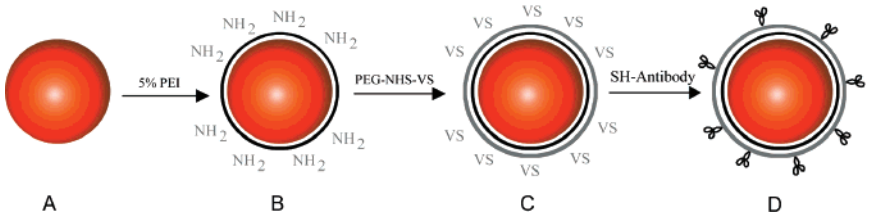

Figure 2. Chemical scheme used to functionalize the red polystyrene particles with antibodies. Bare particles were coated with PEI using physical adsorption (B); the particles were coated with a monolayer of PEG using the hetrobifunctional cross-linker NHS−PEG−VS (C); and thiol functionalized antibodies were immobilized on the PEG monolayer (D).

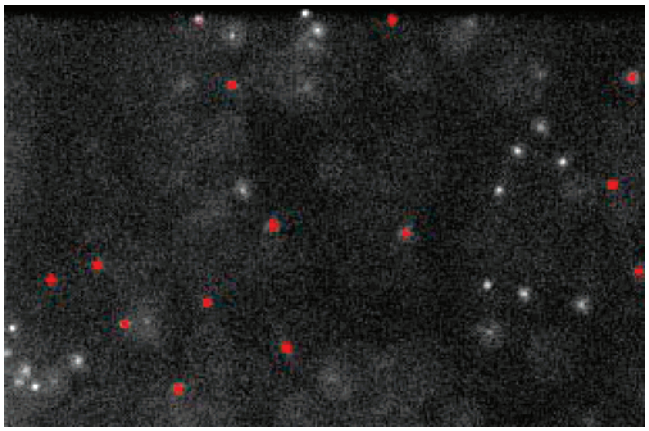

Figure 3. Typical epi-fluorescenc image of a distribution of 4.6×10^8 particles/mL. Only those particles were chosen for analysis (shown in red) that have a maximum intensity is the upper 30th fraction in the image and were at least 10 particle diameters away from any other particle and the walls.

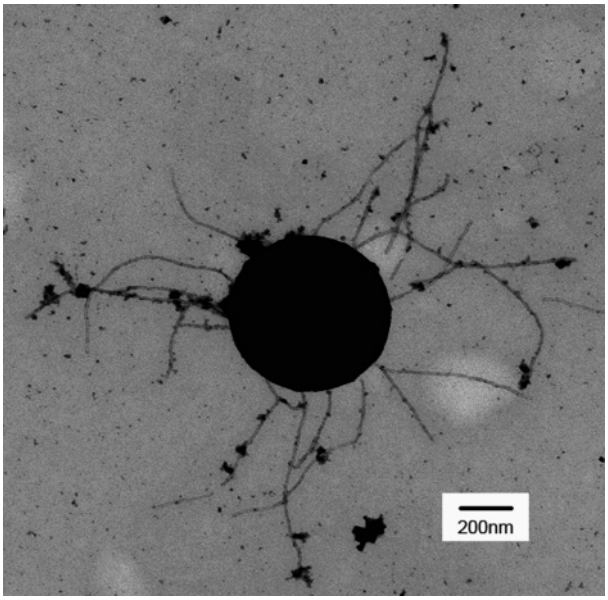

Figure 4. TEM image of a red fluorescent microparticle that has reacted with the M13 virus in a ratio of 1:10. TEM specimens were prepared by floating Formvar and carbon coated TEM grids on droplets of the virus-bead sample. The specimen was then negatively stained with 0.2% uranyl acetate and examined in a field emission TEM (Philips CM-100).

full length from the microparticle. Unfortunately, it was not possible to measure the average length of the phage.

The resolution of the fluorescence particle diffusometry technique was characterized by reacting known concentrations of virus with known densities of particles and monitoring the change in diffusivity of microparticles. The diffusion coefficient of pure suspensions of bare green and anti-pVIII-coated red

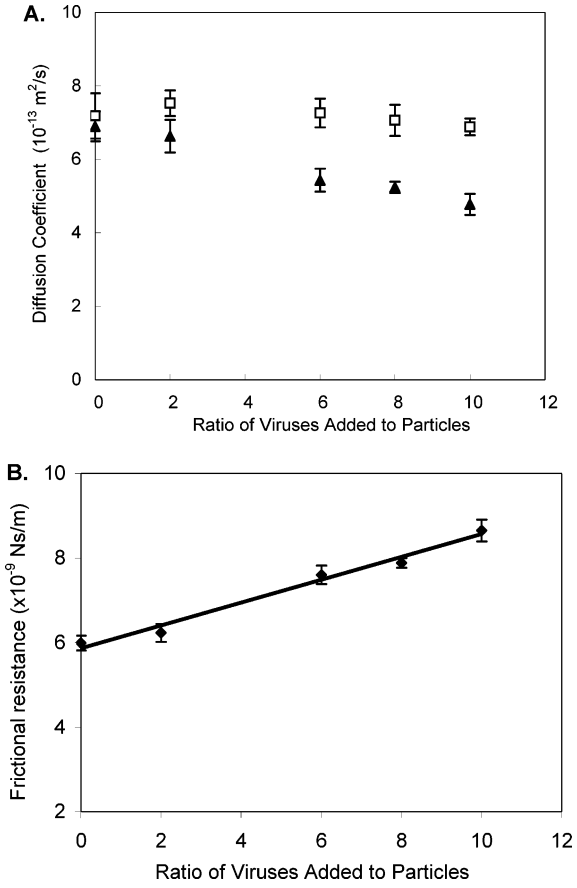

Figure 5. (A) Diffusion coefficients of unmodified (□) and modified (▲) particles measured as function of the concentration of the virus added to the microparticles. Variation in diffusion coefficients of unmodified particles is statistically insignificant while there is a significant decrease in diffusion of modified particles as a function of increasing virus concentrations. (B) Frictional resistance on antibody-functionalized particles measured as a function of virus concentration added to the microparticles.

particles was first measured to be $7.32 \pm 0.23 \times 10^{-13}$ and 7.08×10^{-13} m^2/s, respectively. The mean diffusion coefficient of the particles was determined using the particle tracking algorithm described in the Materials and Methods section. M13 virus was them reacted with 9.2×10^8 anti-pVIII particles particles/mL at a ratio of 1:1, 2:1, 6:1, 8:1, and 10:1 viruses per particle. These reactions were carried out for 30 min in PBS, and then unmodified green microparticles were added to each sample at a concentration of 4.6×10^8 particles/mL. The diffusion coefficients of mixture of antibody-functionalized red particles and unmodified green particles were then measured as a function of M13 concentration. Figure 5A presents the diffusion coefficients measured on microparticles with increasing virus concentrations. The significance of the observed change in the diffusion coefficients of the unmodified green microparticles and antibody-functionalized red microparticles was tested using analysis of variance. The

variation in the diffusion coefficients is not found to be significant for the bare green particles, i.e., the *p*-value was 0.0874. Hence, it appears that increase in virus concentration and other environmental factors do not change the diffusion coefficient of the bare particles in a systematic manner. However, it is clear from Figure 5A that the diffusion coefficient of the antibody-coated red particles decreases systematically as a function of virus concentration, which is confirmed by the *p*-value of 8.6×10^{-8}.

The functional behavior of the decrease in diffusion coefficient as a function of virus concentration was characterized in terms of hydrodynamic drag. The frictional resistance of the particle (ξ) is defined by the Smoluchowski−Einstein[16] theorem to be

$$\xi = \frac{kT}{D} \tag{3}$$

where k is Botzmann's constant and T is temperature. Figure 5B presents the frictional resistance of the anti-pVIII-functionalized particles as a function of the ratio of virus added to the particles. There appears to be a linear relationship between the frictional resistance and number of viruses added per particle (n)

$$\xi = (5.86 + 0.27n) \times 10^{-9} Ns/m$$

Discussion

Interpretation of the Diffusometry Measurements. The measured frictional resistance of the microparticles can be used to characterize their physical properties. That is, if the particles are spherical the frictional resistance is defined by Stokes law to be

$$\xi_s = 6\pi\mu r \tag{4}$$

where r is the radius of the particle and μ is the viscosity of the medium.[17] The frictional resistance of the bare red particles, with no PEG or antibodies, was 5.64×10^{-9} Ns/m, and their hydrodynamic radius was 347 nm, which is in close agreement with the manufacture's specified value. The frictional resistance on an antibody-functionalized particle, with no viruses, was 5.86×10^{-9} Ns/m. The hydrodynamic radius of the particles with the PEI−PEG−IgG layer increases to 361 nm—∼14 nm thicker than the bare particle. The thickness of PEI−PEG films formed on silica surfaces has been measured with ellipsometry to be 6−12 nm.[18] The dimension of the IgG molecule is $10 \times 7 \times 2$ nm^3. Thus, it appears that the increased frictional resistance of the PEI−PEG−IgG-coated particles is consistent with the dense PEI−PEG layer that we have previously established forms on these particles[12] and a submonolayer coverage of IgG.[19]

The frictional resistance of the virus−particle complexes was determined by the number of viruses added to the particles (as described in the Results section). The linear fitting of the frictional resistance data in Figure 5B suggests it results from two contributions: (1) the frictional resistance of the anti-M13-functionalized particle, which was constant at 5.86×10^{-9} Ns/m and (2) the frictional resistance of each virus, which was 2.7×10^{-10} Ns/m. The resistance of the microparticle was in excellent agreement with the measurement made on the particles alone. The frictional resistance of the phage appears to be somewhat more complicated.

The M13 virus will act as a rigid tube in solution as the persistence length of filamentous viruses is of the order of 1 μm.[20] The time-averaged frictional resistance of a prolate ellipsoid traveling with its major axis moving randomly to the direction of flow is

$$\xi_T = \frac{6\pi\mu a}{\ln(2a/b)} \tag{5}$$

where $2a$ is the length of the major axis and $2b$ is one length of the minor axis.[21,22] If the drag of the phage were independent of the microparticle, the overall drag of the phage−virus assembly would simply be the sum of the two contributions

$$\xi = \xi_s + \xi_T \tag{6}$$

Applying these models to the measured frictional resistance of the virus suggests that the average hydrodynamic length of a virus was only 120 nm. This length is significantly shorter than the length of the virus and the apparent structure as determined by electron microscopy (Figure 4). These results suggest that the hydrodynamic drag of the M13 virus was coupled with the microparticle, as expected on the basis of fluid mechanics theory. Coupled hydrodynamic drag coefficients can be determined only by a full calculation of the flow field around a complex assembly of known structure.[23] Unfortunately, a drag coefficient cannot be easily calculated for the virus−particle assembly due to complicated manner in which the viruses are attached to the microparticles.

Influence of Environmental Variables on the Resolution of Particle Imaging Diffusometry. The measurement of diffusion coefficient can be influenced by variations of numerous factors, such as, temperature, viscosity, and particle size. The use of multicolor imaging makes it possible to account for large variations in the factors associated with a specific sample. Variations in temperature can result from the radiation of the light source of the microscope. The uncertainty in the measurement of the diffusion coefficient resulting from temperature fluctuations can be determined from the empirical relation between viscosity and temperature for water[24]

$$\mu = (2.414 \times 10^{-5}) 10^{(247.8/(T-140))} \text{ Ns/m}^2 \tag{7}$$

A change of 0.1 K in the absolute temperature at 299 K decreases the viscosity by 1.97×10^{-6} Ns/m^{2}and increases the diffusion coefficient of particles by 0.034%. Thus, it appears that temperature has a very limited influence on diffusiometry measurements as long as the temperature is controlled to within 1 K.

The viscosity of the medium can also change due to the presence of the particles and free viruses. The presence of particles in a medium changes the viscosity by

$$\mu = \mu(1 + 2.5\phi) \tag{8}$$

where ϕ is the volume fraction of particles and virus. Knowing that the concentration of the particles in the suspension is $4.6 \times$

(16) Einstein, A. *Investigations on the theory of the Brownian movement*; Dover Publications: New York, 1956; p 119.
(17) White, F. M. *Viscous fluid flow*, 3rd ed.; McGraw−Hill Higher Education: New York, 2006; p 629.
(18) Metzger, S. W.; Natesan, M.; Yanavich, C.; Schneider, J.; Lee, G. U. *J. Vac. Sci. Technol. A* **1999**, *17*, 2623−2628.
(19) Shang, H.; Kirkham, P. M.; Myers, T. M.; Cassell, G. H.; Lee, G. U. *J. Magn. Magn. Mater.* **2005**, *293*, 382−388.
(20) Wang, Y. A.; Yu, X.; Overman, S.; Tsuboi, M.; Thomas, G. J.; Egelman, E. H. *J. Mol. Biol.* **2006**, *361*, 209−215.
(21) Berg, H. C. *Random Walks in Biology, Expanded Edition*; Princeton University Press: Princeton, NJ, 1993; p 152.
(22) Perrin, F. *J. Phys. Radium* **1934**, *7*, 497−511.
(23) Berg, H. C.; Turner, L. *Nature* **1979**, *278*, 349−351.
(24) Fox, R. W.; McDonald, A. T.; Pritchard, P. J. *Introduction to fluid mechanics*, 6th ed.; Wiley: Hoboken, NJ, 2004; p 787.

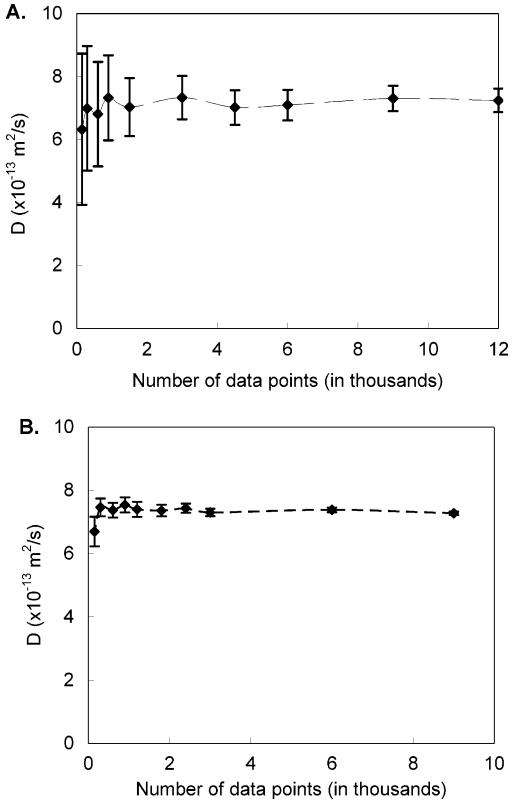

Figure 6. Results of Brownian diffusion simultations. (A) Diffusion coefficients from simulated particle images with a diameter of 690 ± 40 nm. (B) Diffusion coefficients from simulated particle images with a diameter of 690 ± 0 nm.

10^9 per mL, the total volume fraction of the spheres in the sample is calculated to be $\phi = 0.0079$. This number is very small, and hence, the effect of the volume of the spheres on viscosity is also very small. The total volume fraction of viruses is even smaller. Thus, it appears that the variation in viscosity due to the presence of the analyte and microparticles is quite small.

Variation in microparticle size is unavoidable in these measurements as a result of the inherent polydispersity of the microparticles and added variations resulting from PEI−PEG−IgG coating. Brownian diffusion simulations were carried out to understand the effect of particle size variations and the limitations of the particle tracking algorithm on the diffusion coefficient measurements. A mean particle diameter of 690 nm was used with a standard deviation of 40 nm. The Brownian displacement was then calculated for each particle for a given time step. The simulated images were analyzed using the particle tracking algorithm.

Figure 6 presents the results of the Brownian diffusion simulation. The diffusion coefficient and standard deviation were calculated as a function of the number of particle displacements used in the calculation. A total of 9000 data points was analyzed in the experimental measurements presented in each of the measurements reported in this study. The mean value of simulated diffusion coefficient was within 2% of the theoretical value at 9000 data points, and the standard deviation is less than 3%. The combined effect of insufficient data points and limitations in the particle tracking algorithm was explored by performing simulations with a uniform distribution of particles of 690 nm diameter. Figure 6 presents the behavior of diffusion coefficients as a function of the number of data points and the polydispersity of the particle size. At 9000 data points, particle tracking errors accounted for a standard deviation of 1%. These simulations were used to estimate the particle size distribution. We conclude

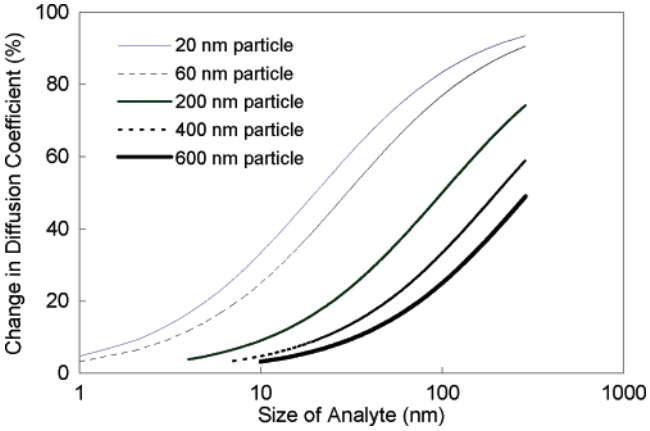

Figure 7. Percentage change in diffusion coefficient of different sized particles as a function of the hydrodynamic radius of the pathogen.

that variation of particle size is the dominant source of variation in the measured diffusion coefficient of the microparticles.

These simulations can be used to estimate the variation in the size of the microparticles. The experimentally measured value of the standard deviation of diffusion coefficient of unmodified red particles was 0.23×10^{-13} m^2/s, whereas the theoretical simulation from Figure 6B is 0.07×10^{-13} m^2/s. If the increase in standard deviation is solely due to the particle size variation, the standard deviation of the diameter of the particle size must be 40 nm.

Resolution of Diffusometry Detection. It is clear that the binding of M13 to a 690 nm diameter antibody-functionalized particle can produce a large enough change in the particle diffusion coefficient that single virus binding events can be detected. However, many analytes are significantly smaller than the M13 virus. We believe that this method can be used to detect these smaller analytes if smaller particles are used. Optical detection and tracking of particles as small as 40 nm is currently possible,[25] which suggests an analyte with a single nanometer-range hydrodynamic radius can be detected.

Figure 7 shows the percentage change in diffusion coefficients of different sized particles as a function of the size of the bound analyte. This figure suggests that a 6 Å diameter analyte will produce a change of 2.9% in the diffusion coefficient of a 20 nm particle, while a pathogen with a hydrodynamic radius of 1 nm will cause a change of 3.23% in the diffusion coefficient of a 60 nm particle. Thus, 0.6−1 nm analytes can in theory be detected with the particle-tracking algorithm that can measure a diffusion coefficient change of 2.3%. This suggests that, with appropriate particles, diffusometry can be used to measure analytes such as ovalbumin, which has a hydrodynamic radius of 1.5 nm. In a previous section of this report, we have demonstrated that the hydrodynamic drag of a large particle with a thin virus are coupled in a complex manner. In the analysis in this paragraph we have assumed that drag is uncoupled, which will result in the overestimation the sensitivity of diffusometry.

Kinetics of the M13 Virus Reaction with the Microparticles. A surprising outcome of this work is that the fluorescent particles did not form cross-linked networks with the virus over the 30 min period in which the reaction was allowed to proceed before analysis was performed. The virus−particle assembly process is controlled by the kinetics of the reaction of the virus with the antibody functionalized fluorescent particles and the rate of interaction of the particles with the virus and each other. The

(25) Csaki, A.; Kaplanek, P.; Moller, R.; Fritzsche, W. *Nanotechnology* **2003**, *14*, 1262−1268.

relative importance of the reaction and diffusion rates in this process may be assessed using dimensional analysis. The dimensionless group that characterizes the dominant processes is the second Damkohler number

$$\frac{k_{on} r_h^{\,2}}{D} \tag{9}$$

where k_{on} is the on-rate of the antibody reaction and r_h is the hydrodynamic radius. The calculated diffusion coefficient of the M13 virus was 3.2×10^{-12} m^2/s. The typical values of k_{on} and k_{off} for antibodies are between 10^3 and 10^4 M^{-1}•s^{-1} and 10^{-2} and 10^{-4} s^{-1}, respectively. This necessarily means that the Damkohler number is much greater than 1 for the antibody concentrations used in this study[18,19] and, thus, the rate of the chemical reaction is much faster than the rate of diffusion.

The image that emerges of the particle−virus reaction is that the virus rapidly reacts with the particle at a rate that is determined by the rate of diffusive transport of the virus to the particles. The relevant time scale for this process is

$$t = \frac{\langle x \rangle^2}{D} \tag{10}$$

where $\langle x \rangle$ is the average distance between the microparticle and virus, which was on the order of 10 μm in the initial reaction volume. The time scale of the virus particle reaction is on the order of 30 s. After this very rapid reaction period, the cross-linking of the microparticles through the virus can take place and if this process is determined by diffusion alone it would take place in less than 140 s. Thus, it appears that diffusion-limited rate of particle−particle reaction is slow but still faster than the observed rate of reaction. We attribute the much slower particle−particle rate of reaction to two phenomena. First, it is known that particle−particle interactions are inhibited by the hydrodynamic resistance that is generated when the particles approach within 10 diameters of each other.[26] Second, the reaction of two particles will be influenced by the spatial alignment of the virus and particles. That is, the reaction will only produce a two-particle complex if the virus is correctly positioned during the collision.

Conclusions

This study demonstrated that binding of analytes to antibody-functionalized particles can be measured using particle tracking algorithms with a high level of sensitivity. The particle diffusometry technique had single virus binding per particle sensitivity, which amounts to about 500 viruses/nL. The high sensitivity of this technique appears to be attractive when compared to current protein detection techniques where significantly more protein is required and multiple antibodies are typically required for signal amplification. There appears to be three practical limitations to implementing this technology. First, in this study large particles have been used which limited the analyte to large viruses. However, if 40 nm particles were used it may be possible to detect analytes as small as 1 nm. Second, the reliability of the particle diffusometry technique was increased by using multicolor particle tracking, which allowed uncoated microparticles to be used to detect changes in environmental parameters, such as temperature and viscosity. This leaves the variation in particle size as the primary source of noise in the measurement. Third, simulations suggest that at least 6000 data points are needed to obtain statistically convergent measurements for uniform-sized particles. It may be difficult to track individual particles for 6000 frames in practice. Thus, it is possible that spot size analysis may be a better way to measure the diffusion coefficients of single molecules based on the diffusional broadening of their optical images.[27]

Acknowledgment. We would like to acknowledge Debbie Sherman for her assistance in preparing the microparticle phage samples for electron microscopy. We would also like to thank Zhigang Wang for providing us with the optical micrograph for Figure 1. Support was provided by the Shreve Trust Purdue University.

LA703224B

(26) Batchelor, G. K.; Wen, C. S. *J. Fluid Mech.* **1982**, *124*, 495−528.

(27) Schuster, J.; Cichos, F.; von Borczyskowski, C. *J. Phys. Chem. A* **2002**, *106*, 5403−5406.

(28) Hovijitra, N.; Lee, S. W.; Shang, H.; Wallis, E.; Lee, G. U. *SPIE Conf. Proc.: Chem. Biol. Sensing V* **2004**, *5416*, 84−93.